Multiple magnetic clouds: Several examples during March–April 2001

Y. M. Wang, P. Z. Ye, and S. Wang
School of Earth and Space Sciences, University of Science and Technology of China, Hefei, China

Received 19 January 2003; revised 30 June 2003; accepted 15 July 2003; published 22 October 2003.

[1] Multiple magnetic cloud (Multi-MC), which is formed by the overtaking of successive coronal mass ejections (CMEs), is a kind of complex structure in interplanetary space. Multi-MC is worthy of notice due to its special properties and potential geoeffectiveness. Using the data from the ACE spacecraft, we identify the three cases of Multi-MC in the period from March to April 2001. Some observational signatures of Multi-MC are concluded: (1) Multi-MC only consists of several magnetic clouds and interacting regions between them; (2) each subcloud in Multi-MC is primarily satisfied with the criteria of isolated magnetic cloud, except that the proton temperature is not as low as that in typical magnetic cloud due to the compression between the subclouds; (3) the speed of solar wind at the rear part of the front subcloud does not continuously decrease, rather increases because of the overtaking of the following subcloud; (4) inside the interacting region between the subclouds, the magnetic field becomes less regular and its strength decreases obviously, and (5) β value increases to a high level in the interacting region. We find out that two of three Multi-MCs are associated with the great geomagnetic storms (Dst ≤ -200 nT), which indicate a close relationship between the Multi-MCs and some intense geomagnetic storms. The observational results imply that theMulti-MC is possibly another type of the interplanetary origin of the large geomagnetic storm, though not all of them have geoeffectiveness. Based on the observations from Solar and Heliospheric Observatory (SOHO) and GOES, the solar sources (CMEs) of these Multi-MCs are identified. We suggest that such successive halo CMEs are not required to be originated from a single solar region. Furthermore, the relationship between Multi-MC and complex ejecta is analyzed, and some similarities and differences between them are discussed. *INDEX TERMS:* 2111 Interplanetary Physics: Ejecta, driver gases, and magnetic clouds; 1739 History of Geophysics: Solar/planetary relationships; 7513 Solar Physics, Astrophysics, and Astronomy: Coronal mass ejections; 2788 Magnetospheric Physics: Storms and substorms; *KEYWORDS:* multiple magnetic clouds, coronal mass ejections, geomagnetic storms, interaction, interplanetary space

Citation: Wang, Y. M., P. Z. Ye, and S. Wang, Multiple magnetic clouds: Several examples during March–April 2001, *J. Geophys. Res.*, *108*(A10), 1370, doi:10.1029/2003JA009850, 2003.

1. Introduction

[2] Statistical studies show that nearly half of all ejecta were comprised by magnetic clouds (MCs) [*Klein and Burlaga*, 1982; *Gosling et al.*, 1992; *Cane et al.*, 1997]. The concept of magnetic cloud was proposed by *Burlaga et al.* [1981]. Enhanced magnetic field strength, long and smooth rotation of magnetic vector, and low proton temperature are the typical features of MC. In all kinds of the interplanetary ejecta, MCs are of most geoeffectiveness [e.g., *Farrugia et al.*, 1997; *Burlaga et al.*, 2001]. On the basis of 17 identifications of great geomagnetic storms during 1972 to 1983, *Burlaga et al.* [1987] concluded that at least 10 (59%) of the events were associated with magnetic clouds. After analyzing 10 intense geomagnetic storms (Dst < -100 nT) near solar maximum (1978–1979), *Tsurutani et al.* [1988] found that four (or five) of the events were related to the magnetic clouds.

[3] In interplanetary space, complex structure exists due to the frequent and intricate solar activities. Generally, complex structure may involve fast shock, magnetic cloud, another high speed stream, corotating stream, and so on [*Burlaga et al.*, 1987; *Behannon et al.*, 1991; *Lepping et al.*, 1997; *Cane and Richardson*, 1997; *Crooker et al.*, 1998; *Knipp et al.*, 1998]. Near solar maximum, coronal mass ejections (CMEs) occur at a rate of ~3.5 events per day [*Webb and Howard*, 1994], and sometimes several CMEs originate from the same solar region within a relatively short interval [e.g., *Nitta and Hudson*, 2001]. Furthermore, CMEs are large-scale structures, especially in interplanetary space. Interaction also may occur between several CMEs in the nearly same directions even though they are not originated from the same region. Thus a complex structure formed due to the overtaking of a series of ejecta is expected in interplanetary medium during the solar maximum.

0148-0227/03/2003JA009850

[4] By analyzing the data from ACE spacecraft during the ascending phase of solar cycle 23, *Burlaga et al.* [2001] divided the fast ejecta excluding corotating stream into two subsets, i.e., magnetic clouds and "complex ejecta." The signatures of ejecta can refer to previous work [e.g., *Bame et al.*, 1981; *Zwickl et al.*, 1983; *Gosling*, 1990, 1997; *Gosling et al.*, 1987; *Richardson and Cane*, 1995; *Neugebauer and Goldstein*, 1997; *Richardson et al.*, 1997]. According to their results, nearly equal numbers of MCs and complex ejecta were found. Compared with magnetic clouds, complex ejecta have disordered weaker magnetic fields, higher proton temperature, and higher ratio of proton thermal pressure to magnetic pressure β on average. The duration of complex ejecta is relatively long (3.1 ± 1.1 days) [*Burlaga et al.*, 2001, 2002]. Nearly all of the complex ejecta have multiple sources. The corresponding geoeffectiveness of the complex ejecta is not apparent because of the absence of ordered magnetic fields which may include extended periods of southward B_z.

[5] Recently, *Wang et al.* [2002a] proposed the concept of multiple magnetic cloud (Multi-MC) in interplanetary space. Multi-MC is formed by the overtaking of successive magnetic clouds and is also one kind of complex interplanetary ejecta. It comprises several relatively isolated subclouds, and each one is primarily satisfied with the criteria of the MC. Due to the relatively regular magnetic fields, Multi-MC can be modeled by flux rope [*Wang et al.*, 2002a]. Since the combinational mode and the number of subclouds in a Multi-MC are various, the situation of Multi-MC can not be enumerated exhaustively. Compared with complex ejecta, some fundamental questions are raised naturally, such as, what are the characteristics of Multi-MC? What is the relationship (or difference) between Multi-MC and complex ejecta? Which conditions are required to form Multi-MC? and Does Multi-MC have strong geoeffectiveness or not?

[6] To understand the properties of Multi-MC, this paper presents three definitive examples during March–April 2001. The ejecta with arbitrary speed are considered when we identify the Multi-MC. Although various signatures of ejecta have been discussed by *Zwickl et al.* [1983], *Gosling* [1990, 1997], *Richardson and Cane* [1995], and *Neugebauer and Goldstein* [1997], there is no definite way to identify ejecta, especially slow ejecta. To guarantee the accuracy of results, we eliminate those ambiguous events.

[7] CMEs are the major sources of such interplanetary ejecta. The characteristics of CME have been studied by many authors [e.g., *Howard et al.*, 1982, 1985; *Hundhausen*, 1988, 1993; *Gosling*, 1990, 1996, 1997; *Low*, 1997; *St. Cyr et al.*, 1999, 2000]. Many CMEs are accompanied by the ejection of filament or the solar flares [*Aly*, 1991; *Wolfson and Low*, 1992; *Wang et al.*, 2002b]. Hence the signatures, such as filament eruption, solar flare, EUV dimming, and so on, can be used to identify the occurrence of CME and find out the corresponding location on solar surface. Halo CME is more important because it points toward or away from the Earth roughly [*Howard et al.*, 1982]. The statistical studies show that nearly half of frontside halo CMEs have geoeffectiveness [*Wang et al.*, 2002b]. Usually, such geoeffective halo CMEs will affect geomagnetic field within 3–5 days [*Webb et al.*, 2000]. As for the extreme large event, the geomagnetic storm may be observed just 1 day after the corresponding CME, for instance, the "Bastille" event [e.g., *Lepping et al.*, 2001; *Smith et al.*, 2001].

[8] In the following three sections, we examine three Multi-MC events during March–April 2001. The observations of these events were collected by the ACE spacecraft. Three primarily characteristics (enhanced magnetic field strength, long and smooth rotation of field vector, and low proton temperature) and other signatures, such as low plasma β (the ratio of proton thermal pressure to magnetic pressure), relatively high density ratio of He^{++} to proton, etc., are referentially used to identify MC. We also study the corresponding disturbances of geomagnetic fields. In addition, we identify the solar sources (CMEs) of these events by using the data from GOES and from LASCO and EIT instruments on board Solar and Heliospheric Observatory (SOHO). In section 5 the observational results are summarized, and a worthy discussion is given.

2. The 3–5 March 2001 Event

[9] Figure 1 shows a complex structure detected by the ACE spacecraft. The structure began at 0505 UT on 4 March 2001. A weak shock was preceding it at 1036 UT on 3 March. The front part of the structure, from 0505 UT to 1205 UT on 4 March, contained a magnetic cloud (MC1). The magnetic field strength was 8.3 nT, relatively higher than the strength of ambient magnetic field (about 4 nT), and magnetic field vector rotated. The proton temperature within it was low although there was no obvious drop of temperature at the front border. The ratio of the density of He^{++} to proton N_α/N_p was relatively high ($\sim$0.1), which indicated the presence of ejecta [*Hirshberg et al.*, 1972; *Ogilvie and Hirshberg*, 1974; *Neugebauer*, 1981; *Neugebauer and Goldstein*, 1997; *Skoug et al.*, 1999]. The average value of plasma β was 0.059, lower than the typical β value of $0.1 \sim 1$ at 1 AU. It was consistent with that for magnetic clouds ($\beta = 0.06 \pm 0.04$) [*Farrugia et al.*, 1993; *Burlaga et al.*, 2001]. Within this MC, the solar wind speed descended slightly. However, the speed increased again at the rear of the cloud (indicated by the solid bar in speed profile of Figure 1). This shows that the rear of the cloud was overtaken and compressed by some structures.

[10] In Figure 1 the overtaking magnetic cloud (MC2) started at 1525 UT, 4 March and ended at 0135 UT, 5 March. Its enhanced magnetic field strength (13.1 nT) was stronger than that of MC1. The cloud characteristics within it were clearer. The long and smooth rotation of field direction, low proton temperature, low β value (0.067 average), and relatively high ratio N_α/N_p existed throughout the cloud. An interacting region was found between the two MCs. Inside that region, magnetic field was less smooth than that in clouds, magnetic field strength reached its minimum, while the β ascended to a high value ($\sim$1.0) again (as marked by a circle in the eighth panel in Figure 1).

[11] MC1, MC2, and the interacting region between them formed the defined Multi-MC. The duration of the Multi-MC was 20.5 hours that had the same order as that of a typical magnetic cloud. A corotating stream can be identified by its ascending speed, relatively low density and high proton temperature [*Hundhausen*, 1972]. We find

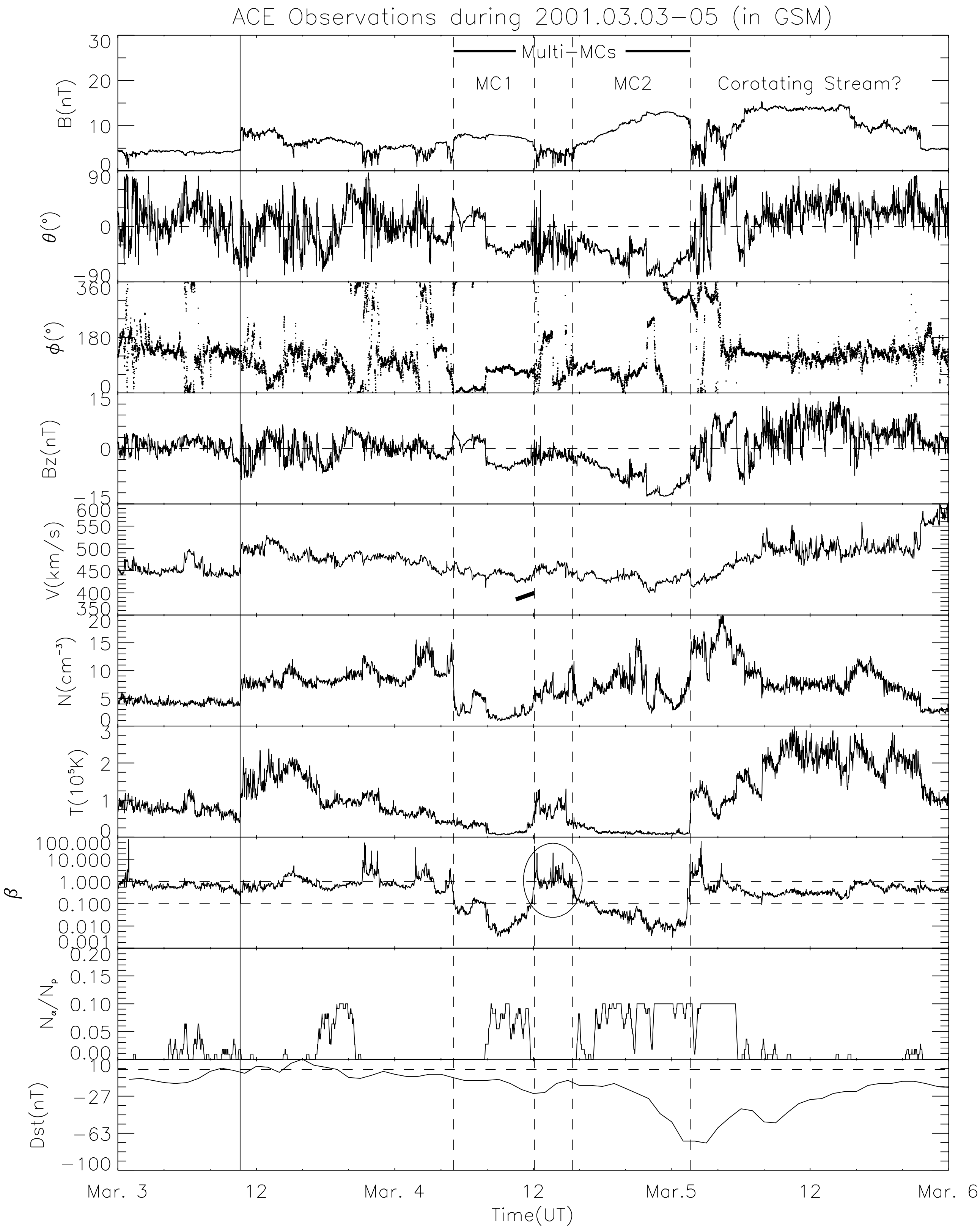

Figure 1. Observations by ACE spacecraft from 3 March to 5 March 2001 (in GSM). From top to bottom are plotted magnetic field strength (B), the elevation (θ) and azimuthal (ϕ) angles of field direction, z component field (B_z), solar wind speed (V), proton density (N), proton temperature (T), the ratio of proton thermal pressure to magnetic pressure (β), the density ratio of He^{++} to proton (N_α/N_p), and geomagnetic index (Dst).

Table 1. Halo CMEs[a] and Associated Solar Activities From 27 February to 3 March 2001

	Date	Time,[b] UT	Speed,[c] km/s	SA[d]	Location	Comments
1	28/02	1450	313	DSF[e]	S17W05	Related to MC1
2	01/03	1826	631	DSF[e]	S33E05	Related to MC2
3	02/03	1006	370	None	–	Backside? EIT data gap

[a]Apparent width of CMEs $\geq 130°$.
[b]The time of the first appearance in LASCO/C2.
[c]Projected speed of CMEs.
[d]Associated solar activities.
[e]DSF means disappearing solar filament.

out that there seems to be a corotating stream following this Multi-MC.

[12] The intensity of geomagnetic storm strongly depends on some interplanetary parameters, such as solar wind speed (V), southward interplanetary magnetic field strength (Bs), the duration of Bs (ΔT), etc. [*Dungey*, 1961; *Snyder et al.*, 1963; *Fairfield and Cahill*, 1966; *Akasofu*, 1981; *Smith et al.*, 1986; *Gonzalez et al.*, 1989, 1994]. Statistical study suggests the threshold values of $Bs \geq 10$ nT and $\Delta T \geq$ 3 hours for intense geomagnetic storms with Dst ≤ -100 nT [*Gonzalez and Tsurutani*, 1987]. The bottom panel of Figure 1 shows the Dst index that presents the disturbance of Earth's magnetosphere. In this event the maximum of magnetic field strength of MC1 was 8.3 nT and the corresponding southward component was not larger than 6 nT. Hence there was no geomagnetic storm observed during this interval. For MC2, the maximum B was 13.1 nT, Bs reached 12.9 nT, and ΔT with $Bs \geq 10$ nT was about 3.5 hours, which met the criteria of creating intense geomagnetic storms. However, MC2 only produced a moderate storm with Dst peak value = -73 nT at 0300 UT on 5 March. The intensity of the storm was less than the expected. *Farrugia et al.* [1998] had quoted such a discrepancy in studying the January 1997 magnetic cloud. Furthermore, it should be noted that the enhanced magnetic field strength B and corresponding B_s within MC2 were caused probably by the compression of the following corotating stream. Thus this Multi-MC's contribution to geoeffectiveness is much smaller.

[13] To identify the solar sources of the interplanetary event, we examine the data from SOHO. The "CME catalog" (available at http://cdaw.gsfc.nasa.gov/CME_list/) is utilized as the reference. We only consider the halo CMEs, whose apparent width in LASCO/C2 were larger than 130° [*Hudson et al.*, 1998] here. Table 1 lists the all candidate halo CMEs from 27 February to 3 March. It is unlikely that CMEs occurring outside this period formed the Multi-MC.

[14] The first CME listed in Table 1 was visible in C2 at 1450 UT on 28 February. Its initial projected speed was about 313 km/s. EIT observed a corresponding quiescent filament eruption just before the CME near disk center at location S17W05. The second CME appeared in C2 at 1826 UT on 1 March with projected speed of 631 km/s. It was also resulted by a quiescent filament erupting at approximate location S33E05. The third CME was first seen in C2 at 1006 UT on 2 March with projected speed of 370 km/s. Unfortunately, there were no EIT observations during the interval of its eruption. There was no filament eruption or solar flare reported either. So this halo CME probably occurred on the backside of the solar disk.

[15] Since there are only two subclouds in this Multi-MC and two appropriate halo CMEs, we derive that the first halo CME results in MC1 and the second CME leads to MC2. Assuming that the projected speed presented the real speed of the CME, the second CME moved faster than the first one. Thus the second CME could overtake the earlier one and form the Multi-MC in interplanetary medium. According to *Cliver et al.* [1990], the relationship between the average transit speed V_t of interplanetary shock from the Sun to 1 AU and the in situ maximum solar wind speed V_{max} follows an empirical equation $V_{max} = 0.775\ V_t - 40$ km/s, roughly. Here, we investigate the shock leading the Multi-MC, which should be associated with the first subcloud inside the Multi-MC. The average transit speed of this shock is 614.8 km/s and consistent with the MCs' in situ maximum solar wind speed of $\sim$470 km/s.

3. The 31 March 2001 Event

[16] This event has been studied in another paper [*Wang et al.*, 2003b, hereinafter referred to as Paper I] recently. The aim of that paper is to discuss that why the Multi-MC caused the largest geomagnetic storm during this solar maximum. Here, our main task is to draw out the characteristics of Multi-MC. In order to keep the integrity of this paper, we describe the event again although it has been presented in [Paper I].

[17] Figure 2 shows a complex structure on 31 March 2001, which began at 0505 UT. Prior to this structure, there was a very intense forward shock at 0020 UT. The first magnetic cloud (MC1) was observed from 0505 UT to 1015 UT. The maximum magnetic field strength B_{max} was 49.1 nT and the southward component B_s reached to 47.9 nT. The density ratio N_α/N_p was 0.1 and β was around 0.074. The duration ΔT with $B_s \geq 10$ nT was nearly 3 hours. Compared with the B_s intrinsic to the MC1, the southward component of the field in the sheath was smaller with some sharp fluctuations. It triggered the geomagnetic storm at around 0400 UT on 31 March. Right after this, the longer and larger B_s event in the cloud MC1 caused the greatest geomagnetic storm with Dst peak value of -387 nT at 0900 UT. During 1235 UT-2140 UT, the spacecraft passed through the second MC (MC2). Within MC2, $\beta \sim 0.075$, $N_\alpha/N_p \sim 0.1$, B_{max}, B_{smax}, and ΔT were equal to 41.4 nT, 36.8 nT, and 7.5 hours, respectively. This event with long duration B_s not only prolonged the great geomagnetic storm but also produced another peak of Dst (-284 nT) at 2200 UT. According to the observations (we examine the entire ACE data in 2001), the proton temperature within typical magnetic cloud is in the order of, even less than, 10^4 K. During these two MCs, the proton temperature was in the order of 10^5 K, one order higher than that of typical magnetic cloud. We believe that the distortion of temperature was caused by the compression between the clouds MC1 and MC2.

[18] The speed profile in Figure 2 shows that the solar wind speed was declining throughout the two MCs, except for a slight increase at the rear of MC1. This signature

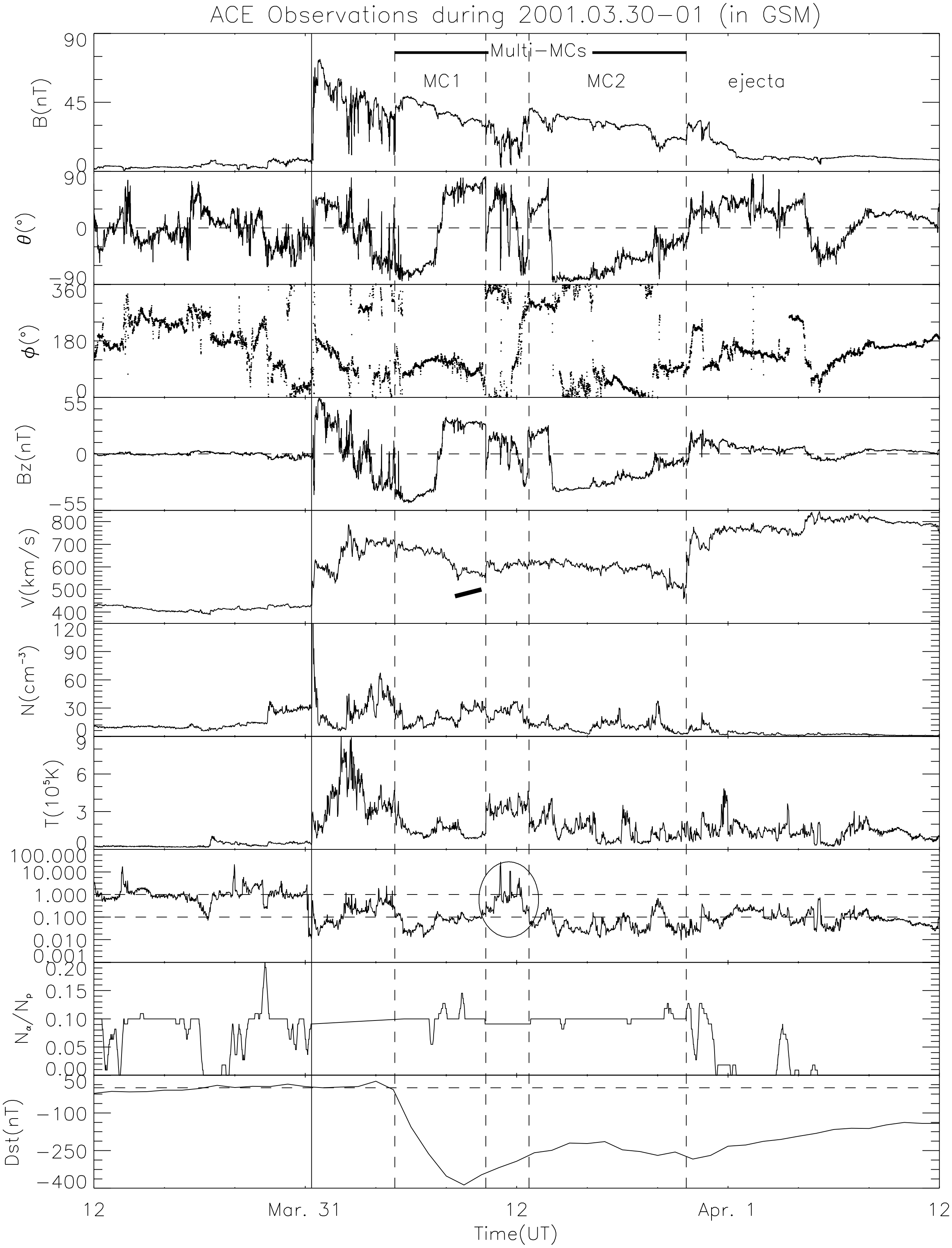

Figure 2. Observations by ACE spacecraft from 1200 UT 30 March to 1200 UT 1 April 2001 (in GSM). From top to bottom are plotted magnetic field strength (*B*), the elevation (θ) and azimuthal (ϕ) angles of field direction, z component field (B_z), solar wind speed (*V*), proton density (*N*), proton temperature (*T*), the ratio of proton thermal pressure to magnetic pressure (β), the density ratio of He^{++} to proton (N_α/N_p), and geomagnetic index (*Dst*). (Taken from *Wang et al.* [2003b])

Table 2. Halo CMEs[a] and Associated Solar Activities From 26 to 30 March 2001

	Date	Time,[b] UT	Speed,[c] km/s	SA[d]	Location	AR[e]	Comments
1	28/03	0127	427	C5.6 flare?	N20E22?	9401?	Related to MC1
2	28/03	1250	519	M4.3 flare	N18E02	9393	Related to MC2
3	29/03	1026	942	X1.7 flare	N20W19	9393	Related to ejecta

[a]Apparent width of CMEs $\geq 130°$.
[b]The time of the first appearance in LASCO/C2.
[c]Projected speed of CMEs.
[d]Associated solar activities.
[e]Solar active region.

implies the compression due to the overtaking of the clouds. In the interacting region located between MC1 and MC2, the magnetic field became less regular and β value approached to 1.0 again. Here, MC1, the interacting region and MC2 were composed of the Multi-MC, which lasted 16.6 hours. Following the Multi-MC, another small ejecta was observed. Its shock arrived at 2140 UT. It is not considered a part of this event because there was a shock between the MC2 and the ejecta and its magnetic field strength was relatively weak. In our definition, there is no other type of structure (e.g., shock) within a Multi-MC except magnetic clouds.

[19] Table 2 lists the all three halo CMEs from 26 to 30 March. The first CME was visible in C2 at 0127 UT on 28 March. Its initial projected speed was about 427 km/s. EIT observations showed some activities on solar surface around the occurrence of the CME. Thus there was ambiguity to identify the CME's source region. According to the observations from GOES about X-ray flares, we think that the CME is associated with a C5.6 X-ray flare (N20E22) which erupted from AR9401 at 0129 UT. The second CME appeared in C2 at 1250 UT on the same day with projected speed of 519 km/s. EIT showed a solar event in AR9393. GOES showed that an M4.3 X-ray flare (N18E02) was exploded at 1121 UT in this active region. The last CME was first seen in C2 at 1026 UT on 29 March with projected speed of 942 km/s. EIT and GOES suggested the CME was associated with a X1.7 X-ray flare (N20W19) beginning at 0957 UT from AR9393.

[20] The intervals between the three CMEs were 11.4 hours and 21.6 hours, respectively. If their projected speeds were representative of the speeds along the Sun-Earth direction, the second CME moved faster than the first one. Therefore it overtook the earlier one and formed a Multi-MC as observed by the ACE. On the other hand, slow CMEs accelerate and fast CMEs decelerate when moving outward [*Gopalswamy et al.*, 2000]. Thus although the initial speed of the last halo CME was much larger than the others, it likely just caught up with the preceding CME because of the too long delay after the second CME's initiation and the probable deceleration in interplanetary space. Hence we suggest that the first two CMEs are related to the two subclouds in the Multi-MC and the last CME corresponds to the ejecta, which follow the Multi-MC but do not interact with it sufficiently yet at 1 AU. The transit speed of the shock leading the Multi-MC is 587.8 km/s and not consistent with the maximum solar wind speed of 710 km/s based on the *Cliver et al.* [1990] equation. Even if the leading shock is associated with the second subcloud, its transit speed is 700.3 km/s, which is also not very consistent with the insitu maximum solar wind speed.

4. The 11–13 April 2001 Event

[21] The complex structure shown in Figure 3 began at 2215 UT on 11 April 2001. There were two shocks preceding the structure at 1312 UT and 1527 UT, respectively. The front part of the structure, from 2215 UT, 11 April to 0355 UT, 12 April, was a magnetic cloud (MC1) due to its enhanced magnetic field strength (35.5 nT, much higher than the interplanetary field strength ~5 nT), smooth rotation of field vector, low β value (~0.078), and relatively high density ratio N_α/N_p (nearly 0.1). Although the proton temperature was higher than that for a typical magnetic cloud, we believe that the relatively high temperature was caused by the compression between the clouds. The interaction of MC with other ejecta distorted some signatures of magnetic cloud that made it more difficult to identify the MC. This cloud, in which the maximum Bs = 34 nT and $\Delta T \sim 2$ hours, caused a great geomagnetic storm by combining the shock sheath before it. Dst peak was −271 nT at 2400 UT on 11 April. The second MC (MC2) was observed from 0805 UT, 12 April to 0705 UT, 13 April. The characteristics of MC2 were evident: B_{max} = 20.6 nT, $\beta \sim 0.014$, and $N_\alpha/N_p \sim 0.1$. The magnitude of magnetic field was lower than that in MC1. Since the z-component of magnetic field was almost northward direction, there was no more geomagnetic storm following it.

[22] Between the two clouds, an interacting region also existed. The first cloud MC1 lasted about 5.7 hours, much less than the average. It can be considered the result of the overtaking and compressing between the clouds. Some smaller-scale magnetic clouds have ever been reported by *Crooker et al.* [1996] and *McAllister et al.* [1998]. The Multi-MC consisting of two MCs and one interacting region continued for 32.8 hours. After the Multi-MC, there was the third MC (MC3) from 1230 UT, 13 April to 1005 UT, 14 April. Its shock arrived at 0705 UT on 13 April. We exclude MC3 from this Multi-MC event because there was a shock between MC2 and MC3 that did not satisfy our definition of Multi-MC.

[23] All of the four halo CMEs from 8 to 11 April are listed in Table 3. They are all Earth-directed by examining the data from SOHO and GOES. If MC1 was formed by the first CME, the transit speed of the CME was about 590 km/s and it was too slow to own such high in situ solar wind speed. We conclude that the second CME is related to MC1 with its average transit speed of 770 km/s, the third CME is related to MC2 with its transit speed of 820 km/s, and the fourth one is related to MC3 with its transit speed of 890 km/s. Related the first leading shock to the first subcloud, the average transit speed of this shock is 919.8 km/s, consistent with the in situ maximum solar wind speed of 740 km/s [*Cliver et al.*, 1990].

5. Summary and Discussion

[24] We have studied the three events about Multi-MC during March–April 2001 (within the solar maximum of cycle 23). According to the above analyses, we conclude the following definite characteristics of Multi-MC: (1) as the definition, Multi-MC only consists of the magnetic clouds

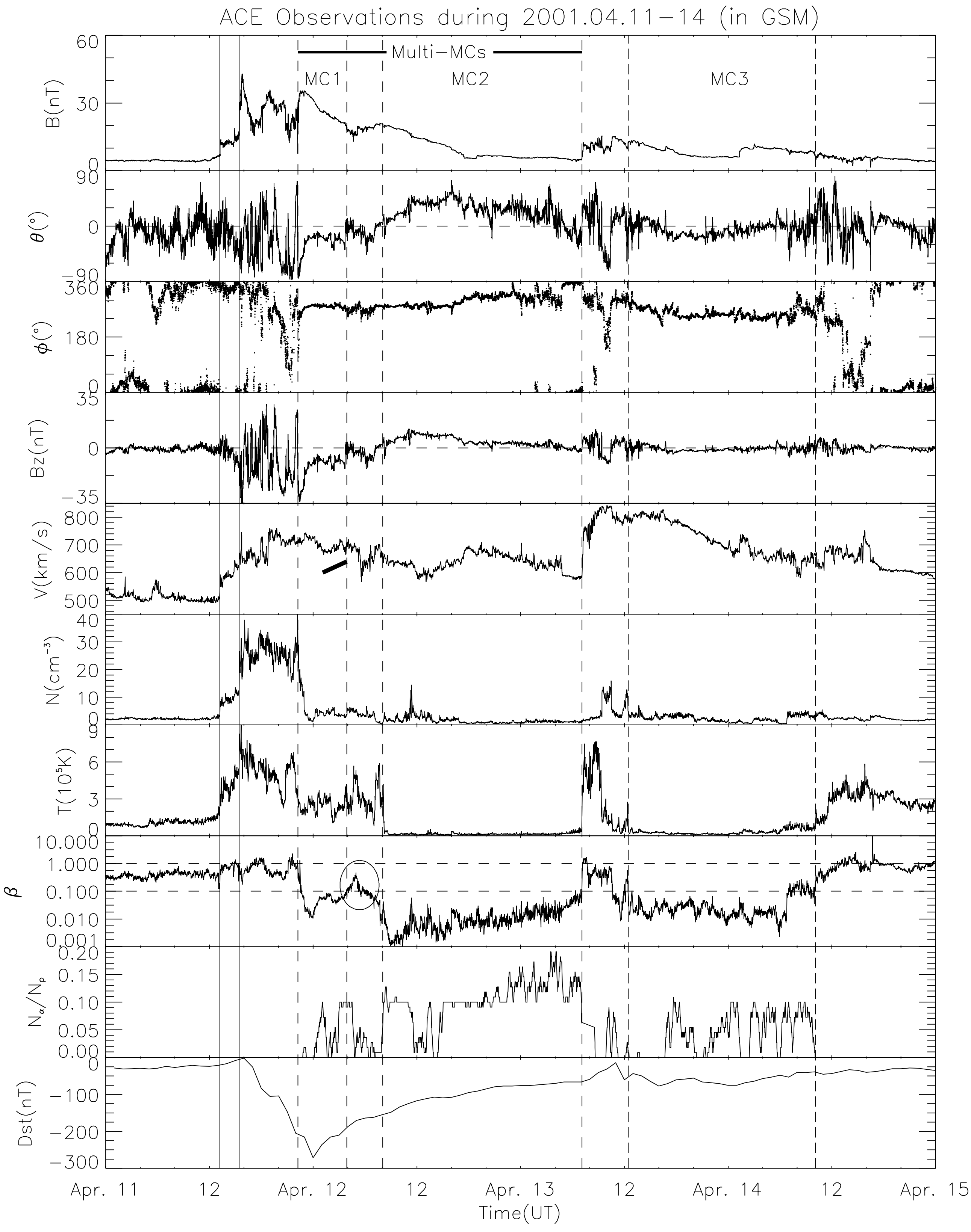

Figure 3. Observations by ACE spacecraft from 11 April to 14 April 2001 (in GSM). From top to bottom are plotted magnetic field strength (B), the elevation (θ) and azimuthal (ϕ) angles of field direction, z component field (B_z), solar wind speed (V), proton density (N), proton temperature (T), the ratio of proton thermal pressure to magnetic pressure (β), the density ratio of He^{++} to proton (N_α/N_p), and geomagnetic index (Dst).

Table 3. Halo CMEs[a] and Associated Solar Activities From 8 to 11 April 2001

	Date	Time,[b] UT	Speed,[c] km/s	SA[d]	Location	AR[e]	Comments
1	09/04	0006	653	EUV dimming	S25E16	9415?	
2	09/04	1554	1192	M7.9 flare	S21W04	9415	Related to MC1
3	10/04	0530	2411	X2.3 flare	S23W09	9415	Related to MC2
4	11/04	1332	1103	M2.3 flare	S22W27	9415	Related to MC3

[a]Apparent width of CMEs $\geq 130°$.
[b]The time of the first appearance in LASCO/C2.
[c]Projected speed of CMEs.
[d]Associated solar activities.
[e]Solar active region.

and the interacting regions between them; (2) each subcloud in Multi-MC satisfies the criteria of isolated magnetic cloud, except that proton temperature is sometimes not as low as that in typical magnetic cloud. We believe that the distortion of proton temperature is resulted from the interaction between the subclouds. Under the effect of the compression, the proton temperature in Multi-MC will somewhat increase but the corresponding β value is still low; (3) solar wind speed at the rear of overtaken cloud does not decline continuously, but rather increases because of the compressing by the overtaking cloud behind; (4) within the interacting region, the magnetic field becomes less regular, its strength drops to minimum, and (5) β value increases to a high level.

[25] In above examples, the duration of Multi-MCs are 20.5, 16.6, and 32.8 hours, respectively. These values are comparable to the duration of typical magnetic clouds. Comparing the duration of the subclouds, we find that the time of the second cloud is longer than the first in all cases. The duration of MC1 and MC2 in three events are (7.0, 10.2), (5.2, 9.1), and (5.7, 23.0) hours, respectively (as listed in the fourth column of Table 4). It implies that the compression degree of subclouds in Multi-MC is different, and the former subcloud gets the more compression.

[26] These three events are all associated with geomagnetic storms. On the basis of the observations, the 5 March geomagnetic storm seems to be irrelevant to the Multi-MC. It is caused by the compression between the corotating stream and the preceding cloud (MC2). In the second event, the magnetic field strength is extraordinary large due to the interaction of the subclouds. The enhanced southward field B_s in MC1 should be the main factor to generate the great geomagnetic storm on 31 March. Similarly, in the third event, the MC1 has the strong magnetic field due to the overtaking of the second cloud MC2. The combination between the shock sheath before MC1 and the compressed B_s within MC1 produced the great geomagnetic storm on 12 April. The reason why the first Multi-MC does not contribute to the geoeffectiveness may be that the subclouds within the Multi-MC are too faint and the corresponding fields magnitude therefore are small (around 10 nT approximately) in despite of the presence of the interaction between the subclouds. For the second and third Multi-MC, we believe that the large magnetic fields strength are mainly resulting from the compression of these subclouds. However, there are only three cases analyzed, and not all of the Multi-MCs can result in the moderate to intense geomagnetic storms. It is thus still difficult to conclude quantitatively the effect of Multi-MC on Earth's magnetosphere.

[27] On the other hand, the interplanetary cause of great geomagnetic storms is various, such as large magnetic cloud, field draping, shock compression, and so on [*Gosling and McComas*, 1987; *Tsurutani et al.*, 1992; *Wang et al.*, 2003a]. During the investigated 2 months, from March to April, there are only two great geomagnetic storms with $Dst \leq -200$ nT or five intense storms with $Dst \leq -100$ nT. Undoubtedly, all of the great storms or 2 of 5 intense storms are associated with the Multi-MCs, which imply the close relationship between large geomagnetic storms and Multi-MCs. Hence we suspect that the Multi-MC is possibly another type of the important interplanetary origin of the large geomagnetic storm though some Multi-MCs are of little geoeffectiveness. This idea has been suggested in recent work [Paper I].

[28] The analyses of solar sources for Multi-MCs show that each subcloud in Multi-MCs can be related to a halo CMEs generally. Due to the overtaking between the CMEs, the relationship between the maximum solar wind speed and the transit speed of CME's leading shock $0.55 \leq V_{max}/V_t \leq 0.93$, derived by *Cliver et al.* [1990], is not suitable for the Multi-MCs. In the second case, V_{max} is larger than the corresponding V_t. Due to the overtaking and interacting between successive halo CMEs, their propagations become more uncertain and intricate. In addition, these successive halo CMEs may not be required to occur in the same solar region although the CMEs listed in the third case are located in the same active region. The two selected CMEs, in the

Table 4. Multi-MCs Observational and Model Fit Parameters

Events, date	No.	B,[a] nT	T,[b] hours	B_0,[c] nT	H[d]	R_0,[e] AU	θ[f]	φ[g]	t_c,[h] hours	D^i/R_0	χ^2	Correlation
3–5 March	1	7.5	7.0	6.1	1	0.032	−31°	270°	2.4	0.468	0.249	0.90
	2	10.0	10.2	10.0	−1	0.088	−87°	177°	8.0	0.169		
31 March	1	39.1	5.2	64.7	1	0.044	−54°	134°	1.6	0.353	0.191	0.84
	2	29.7	9.1	33.5	1	0.084	−55°	315°	1.7	0.310		
11–13 April	1	26.1	5.7	27.9	−1	0.029	−83°	257°	0.3	0.290	0.103	0.94
	2	9.2	23.0	15.0	−1	0.164	−20°	266°	−1.5	0.096		

[a]Observed average magnetic field strength of MC.
[b]Duration of MC.
[c]Axial field magnitude.
[d]The sign of cloud's helicity, 1 indicates right-handedness and -1 indicates left-handedness.
[e]Radius of cloud.
[f]Latitude of cloud axis, GSM.
[g]Longitude of cloud axis, GSM.
[h]Center time from start of cloud.
[i]The closest approach distance from the axis of the cloud.

first case, are both generated by filament eruption at the different locations, where are out of active regions. In the second case, the two CMEs, which are probably originated from the different active regions, formed the Multi-MC at 1 AU on 31 March 2001.

[29] The developed constant-alpha force-free flux rope model of Multi-MC has been proposed by *Wang et al.* [2002a]. They simply applied the linear combination of isolated flux rope to model the Multi-MC. Instead of fitting the subclouds one by one, we use the Multi-MC model to fit the observations because the effect of magnetic fields between the subclouds should not be ignored.

[30] Fitting of isolated magnetic cloud by force-free flux rope model has ever been studied by some authors [e.g., *Burlaga*, 1988; *Lepping et al.*, 1990]. The method of fitting Multi-MCs is similar. To fit all three components of magnetic field, seven parameters need to be determined: (1) B_0, magnetic field strength on the axis of the cloud, (2) $H = \pm 1$, the sign of the helicity, (3) R_0, the radius of the cloud, (4) θ and (5) ϕ, the latitude and longitude of the cloud's axis (respect the ecliptic plane), (6) t_c, center time at the closest approach to the cloud's axis, and (7) D, the distance of the spacecraft from the cloud axis at closest approach point. We make half-hourly average data and apply a least-squares program [*Marquardt*, 1963] to fit observations. The following equation is adopted to evaluate the goodness-of-fit.

$$\chi^2 = \sum \left[\left(B_x - B_x^f\right)^2 + \left(B_y - B_y^f\right)^2 + \left(B_z - B_z^f\right)^2 \right] / N,$$

where the superscript "f" indicates the fitting data of magnetic fields, and N is the number of field vectors. The B and B^f are unit normalized. Table 4 lists the results of the model fitting to the measured fields.

[31] The value of χ^2 is 0.249, 0.191, and 0.103, respectively, and the corresponding correlation coefficient is 0.90, 0.84, and 0.94. These low χ^2 and high correlation coefficients indicate the good fitting. Thus it is feasible to theoretically analyze Multi-MC by using this model.

[32] According to Table 4, the estimated diameter of the leading subcloud is $\sim$0.07 AU on average, smaller than that of the trailing subcloud. The result also implies that the compression degree of subclouds in Multi-MC is different, and the leading subcloud gets more compression. This conclusion is consistent with what obtained in the second paragraph in this section. The direction of the subcloud's axis varies, and even in the same Multi-MC, the subclouds may be oriented differently. The second subcloud of 3–5 March Multi-MC and the first subcloud of 11–13 April Multi-MC are almost perpendicular to the ecliptic plane, and others are all inclined to the ecliptic plane. The axes of the subclouds within the first and third Multi-MC are perpendicular to each other, and the subclouds within the second Multi-MC are antiparallel. The difference orientation of the subclouds' axes rise the variety and complexity of the Multi-MC. In addition, the sign of helicity of the subclouds within a Multi-MC may be different. It lies on the helicity of its solar origin. A further study can be carried out to examine the helicity consistency of the Multi-MCs with their counterpart on the Sun.

[33] If the effect of expansion of magnetic cloud is considered, the observed center of magnetic cloud should approach to its front [*Farrugia et al.*, 1995; *Osherovich and Burlaga*, 1997]. In these cases, this effect is somewhat weak due to the fact that the solar wind speed within almost all of these subclouds is approximately flat, which indicates the small expansion of subclouds. However, from the fitting results, the center of subclouds is all largely shifted to the beginning of subclouds, except the second subcloud in the first Multi-MC. It implies that the compression of the front part of subcloud is usually greater than that of the rear part. It is reasonable that the front part of the overtaking MC is compressed more than the rear of it. However, why does the leading MC, which is overtaken, also present this characteristic? This model is too simple to study Multi-MCs in detail.

[34] Multi-MCs can be considered a subset (or a part) of complex ejecta, which was proposed by *Burlaga et al.* [2001]. They are both formed by several interplanetary structures. However, it can be seen from the above discussions that Multi-MC is different from other types of complex ejecta. Due to Multi-MC's special properties and potential geoeffectiveness, it is worthy to be extracted from complex ejecta for detailed studies. In the papers of *Burlaga et al.* [2001, 2002], the hour-average data was used to identify the complex ejecta. However, for the second case, there are only 5 data points in the first subcloud if hour-average data set is adopted. Hence such resolution is too rough to distinguish Multi-MCs sometimes. Compared with Multi-MCs, other kinds of complex ejecta generally have much larger scale. Their magnetic fields are usually unordered, therefore almost no obvious geomagnetic storms follow them. On the contrary, Multi-MCs have the scale as order as that of MCs. The magnetic fields in Multi-MCs are relatively regular and intense geomagnetic storms sometimes can be expected.

[35] In summary, we have discussed the characteristics of Multi-MCs and suggested that they probably have important effect on the Earth's magnetosphere. The solar sources of Multi-MCs are identified and analyzed preliminarily. The similarities and differences between Multi-MCs and complex ejecta are also discussed. Identifying two or more magnetic clouds in a complex interplanetary structure is difficult because the interactions between ejecta/clouds may distort the signatures of typical magnetic cloud. Furthermore, the difficulty of identifying Multi-MCs becomes even more evident when the observing satellite crosses the clouds very far from its center [*Tsurutani and Gonzalez*, 1997]. Finally, there are still many questions unsolved. For example, which conditions are required for CMEs to form Multi-MCs? How does the overtaking CME interact with the earlier emitted CME in detail? What is the picture of the propagation of Multi-MC? How to predict the geoeffectiveness of Multi-MCs? These all need to be studied further.

[36] **Acknowledgments.** We acknowledge the use of the data from ACE, SOHO, GOES spacecraft, and the Dst index from World Data Center. We thank the anonymous referees for the constructive comments. This work is supported by the National Natural Science Foundation of China (49834030), the State Ministry of Science and Technology of China (G2000078405), and the Chinese Academy of Sciences (KZCX2-SW-136).

[37] Shadia Rifai Habbal thanks Charles John Farrugia and Ian G. Richardson for their assistance in evaluating this paper.

References

Akasofu, S.-I., Energy coupling between the solar wind and the magnetosphere, *Space Sci. Rev.*, *28*, 121, 1981.

Aly, J. J., How much energy can be stored in a three-dimensional force-free magnetic field?, *Appl. J.*, *375*, L61, 1991.

Bame, S. J., J. R. Asbridge, W. C. Feldman, J. T. Gosling, and R. D. Zwickl, Bi-directional streaming of solar wind electrons greater-than 80 eV - ISEE: Evidence for a closed-field structure within the driver gas of an interplanetary shock, *Geophys. Res. Lett.*, *8*, 173, 1981.

Behannon, K. W., L. F. Burlaga, and A. Hewish, Structure and evolution of compound streams at $\leq$1 AU, *J. Geophys. Res.*, *96*, 21,213, 1991.

Burlaga, L. F., Magnetic clouds: Constant alpha force-free configurations, *J. Geophys. Res.*, *93*, 7217, 1988.

Burlaga, L., E. Sittler, F. Mariani, and R. Schwenn, Magnetic loop behind an interplanetary shock: Voyager, Helios, and IMP 8 observations, *J. Geophys. Res.*, *86*, 6673, 1981.

Burlaga, L. F., K. W. Behannon, and L. W. Klein, Compound stream, magnetic clouds, and major geomagnetic storms, *J. Geophys. Res.*, *92*, 5725, 1987.

Burlaga, L. F., R. M. Skoug, C. W. Smith, D. F. Webb, T. H. Zurbuchen, and A. Reinard, Fast ejecta during the ascending phase of solar cycle 23: ACE observations, 1998–1999, *J. Geophys. Res.*, *106*, 20,957–20,977, 2001.

Burlaga, L. F., S. P. Plunkett, and O. C. St. Cyr, Successive CMEs and complex ejecta, *J. Geophys. Res.*, *107*(A10), 1266, doi:10.1029/2001JA000255, 2002.

Cane, H. V., and I. G. Richardson, What caused the large geomagnetic storm of November 1978?, *J. Geophys. Res.*, *102*, 17,445, 1997.

Cane, H. V., I. G. Richardson, and G. Wibberenz, Helios 1 and 2 observations of particle decreases, ejecta, and magnetic clouds, *J. Geophys. Res.*, *102*, 7075–7086, 1997.

Cliver, E. W., J. Feynman, and H. B. Garrett, An estimate of the maximum speed of the solar wind, 1938–1989, *J. Geophys. Res.*, *95*, 17,103–17,112, 1990.

Crooker, N. U., A. J. Lazarus, R. P. Lepping, K. W. Ogilvie, J. T. Steinberg, A. Szabo, and T. G. Onsager, A two-stream, four-sector, recurrance patten: Implications from WIND for the 22-year geomagnetic activity cycle, *Geophys. Res. Lett.*, *23*, 1275–1278, 1996.

Crooker, N. V., J. T. Gosling, and S. W. Kahler, Magnetic clouds at sector boundaries, *J. Geophys. Res.*, *103*, 301, 1998.

Dungey, J. R., Interplanetary magnetic field and auroral zones, *Phys. Rev. Lett.*, *6*, 47, 1961.

Fairfield, D. H., and L. J. Cahill, Transition region magnetic field and polar magnetic disturbances, *J. Geophys. Res.*, *71*, 155, 1966.

Farrugia, C. J., L. F. Burlaga, V. A. Osherovich, I. G. Richardson, M. P. Freeman, R. P. Lepping, and A. J. Lazarus, A study of an expanding interplanetary magnetic cloud and its interaction with the Earth's magnetosphere: The interplanetary aspect, *J. Geophys. Res.*, *98*, 7621, 1993.

Farrugia, C. J., V. A. Osherovich, and L. F. Burlaga, Magnetic flux rope versus the spheromak as models for interplanetary magnetic clouds, *J. Geophys. Res.*, *100*, 12,293, 1995.

Farrugia, C. J., L. F. Burlaga, and R. P. Lepping, Magnetic clouds and the quiet/storm effect at Earth: A review, in *Magnetic Storms*, *Geophys. Monogr. Ser.*, vol. 98, edited by B. T. Tsurutani et al., p. 91, AGU, Washington, D. C., 1997.

Farrugia, C. J., et al., Geoeffectiveness of three WIND magnetic clouds: A comparative study, *J. Geophys. Res.*, *103*, 17,261, 1998.

Gonzalez, W. D., and B. T. Tsurutani, Criteria of interplanetary parameters causing intense magnetic storms (Dst < −100 nT), *Planet. Space Sci.*, *35*, 1101, 1987.

Gonzalez, W. D., B. T. Tsurutani, A. L. C. Gonzalez, E. J. Smith, F. Tang, and S. I. Akasofu, Solar wind-magnetosphere coupling during intense magnetic storms (1978–1979), *J. Geophys. Res.*, *94*, 8835, 1989.

Gonzalez, W. D., J. A. Joselyn, Y. Kamide, H. W. Kroehl, G. Rostoker, B. T. Tsurutani, and V. M. Vasyliunas, What is a geomagnetic storm?, *J. Geophys. Res.*, *99*, 5771, 1994.

Gopalswamy, N., A. Lara, R. P. Lepping, M. L. Kaiser, D. Berdichevsky, and O. C. St. Cyr, Interplanetary acceleration of coronal mass ejections, *Geophys. Res. Lett.*, *27*, 145, 2000.

Gosling, J. T., Coronal mass ejections and magnetic flux ropes in interplanetary space, in *Physics of Magnetic Flux Ropes*, *Geophys. Monogr. Ser.*, vol. 58, edited by C. T. Russell, E. R. Priest, and L. C. Lee, pp. 343–364, AGU, Washington, D. C., 1990.

Gosling, J. T., Corotating and transient solar wind flows in three dimensions, *Annu. Rev. Astron. Astrophys.*, *34*, 35–73, 1996.

Gosling, J. T., Coronal mass ejections: An overview, in *Coronal Mass Ejections*, *Geophys. Monogr. Ser.*, vol. 99, edited by N. Crooker, J. A. Joselyn, and J. Feynman, pp. 9–16, AGU, Washington, D. C., 1997.

Gosling, J. T., and D. J. McComas, Field line draping about fast coronal mass ejecta: A source of strong out-of-the-ecliptic interplanetary magnetic fields, *Geophys. Res. Lett.*, *14*, 355–358, 1987.

Gosling, J. T., D. N. Baker, S. J. Bame, W. C. Feldman, R. D. Zwickl, and E. J. Smith, Bidirectional solar wind electron heat flux events, *J. Geophys. Res.*, *92*, 8519, 1987.

Gosling, J. T., S. J. McComas, J. L. Phillips, and S. J. Bame, Counterstreaming solar wind halo electron events: Solar-cycle variations, *J. Geophys. Res.*, *97*, 6531–6535, 1992.

Hirshberg, J., S. J. Bame, and E. E. Robbins, Solar flares and helium enrichments, *Solar Phys.*, *23*, 467, 1972.

Howard, R. A., D. J. Michels, N. R. Sheeley, and M. J. Koomen, The observation of a coronal transient directed at Earth, *Astrophys. J.*, *263*, L101–L104, 1982.

Howard, R. A., N. R. Sheeley, M. J. Koomen, and D. J. Michels, Coronal mass ejections: 1979–1981, *J. Geophys. Res.*, *90*, 8173–8191, 1985.

Hudson, H. S., J. R. Lemen, O. C. St. Cyr, A. C. Sterling, and D. F. Webb, X-ray coronal changes during CMEs, *Geophys. Res. Lett.*, *25*, 2481–2484, 1998.

Hundhausen, A. J., *Coronal Expansion and Solar Wind*, Springer-Verlag, New York, 1972.

Hundhausen, A. J., The origin and propagation of coronal mass ejections, in *Solar Wind Six*, edited by V. Pizzo, T. E. Holzer, and D. G. Simes, *Tech. Note NCAR/TN-306+Proc.*, pp. 181–214, Natl. Cent. for Atmos. Res., Boulder, Colo., 1988.

Hundhausen, A. J., Sizes and locations of coronal mass ejections-SMM observations from 1980 and 1984–1989, *J. Geophys. Res.*, *98*, 13,177–13,200, 1993.

Klein, L. W., and L. F. Burlaga, Interplanetary magnetic clouds at 1 AU, *J. Geophys. Res.*, *87*, 613–624, 1982.

Knipp, D. J., et al., An overview of the early November 1993 geomagnetic storm, *J. Geophys. Res.*, *103*, 26,197, 1998.

Lepping, R. P., J. A. Jones, and L. F. Burlaga, Magnetic field structure of interplanetary magnetic clouds at 1 AU, *J. Geophys. Res.*, *95*, 11,957–11,965, 1990.

Lepping, R. P., et al., The Wind magnetic cloud and events of October 18–20, 1995: Interplanetary properties and as triggers for geomagnetic activity, *J. Geophys. Res.*, *102*, 14,049–14,064, 1997.

Lepping, R. P., et al., The Bastille Day magnetic clouds and upstream shocks: Near-Earth interplanetary observations, *Sol. Phys.*, *204*, 285, 2001.

Low, B. C., The role of coronal mass ejections in solar activity, in *Coronal Mass Ejections*, *Geophys. Monogr. Ser.*, vol. 99, edited by N. Crooker, J. A. Joselyn, and J. Feynman, p. 39, AGU, Washington, D. C., 1997.

Marquardt, D. W., An algorithm for least-squares estimation of nonlinear parameters, *J. Soc. Ind. Appl. Math.*, *11*, 431, 1963.

McAllister, A. H., D. J. Knipp, N. U. Crooker, T. Mukai, and S. Kokubun, Identification of solar drivers: The November 3–4, 1993, geomagnetic storm, *J. Geophys. Res.*, *103*, 26,221–26,233, 1998.

Neugebauer, M., Observations of solar wind helium, *Fundam. Cosmic Phys.*, *7*, 131, 1981.

Neugebauer, M., and R. Goldstein, Particle and field signatures of coronal mass ejections in the solar wind, in *Coronal Mass Ejections*, *Geophys. Monogr. Ser.*, vol. 99, edited by N. Crooker, J. A. Joselyn, and J. Feynman, p. 245, AGU, Washington, D. C., 1997.

Nitta, N. V., and H. S. Hudson, Recurrent flare/CME events from an emerging flux region, *Geophys. Res. Lett.*, *28*, 3801–3804, 2001.

Ogilvie, K. W., and J. Hirshberg, Solar-cycle variation of solar-wind helium abundance, *J. Geophys. Res.*, *79*, 4595–4602, 1974.

Osherovich, V. A., and L. F. Burlaga, Magnetic clouds, in *Coronal Mass Ejections*, *Geophys. Monogr. Ser.*, vol. 99, edited by N. Crooker, J. A. Joselyn, and J. Feynman, pp. 157–168, AGU, Washington, D. C., 1997.

Richardson, I. G., and H. V. Cane, Regions of abnormally low proton temperature in the solar wind (1965–1991) and their association with ejecta, *J. Geophys. Res.*, *100*, 23,397–23,412, 1995.

Richardson, I. G., C. J. Farrugia, and H. V. Cane, A statistical study of the behavior of the electron temperature in ejecta, *J. Geophys. Res.*, *102*, 4691–4699, 1997.

Skoug, R. M., et al., A prolonged He^+ enhancement within a coronal mass ejection in the solar wind, *Geophys. Res. Lett.*, *26*, 161–164, 1999.

Smith, E. J., J. A. Slavin, R. D. Zwickl, and S. J. Bame, Shocks and storm sudden commencements, in *Solar Wind-Magnetosphere Coupling*, edited by Y. Kamide and J. A. Slavin, pp. 345–365, Terra Sci., Tokyo, 1986.

Smith, C. W., et al., ACE observations of the Bastille Day 2000 interplanetary disturbances, *Sol. Phys.*, *204*, 227, 2001.

Snyder, C. W., M. Neugebauer, and V. R. Rao, The solar wind velocity and its correlation with solar and geomagnetic activity, *J. Geophys. Res.*, *68*, 6361, 1963.

St. Cyr, O. C., J. T. Burkepile, A. J. Hundhausen, and A. R. Lecinski, A comparison of ground-based and spacecraft observations of coronal mass ejections from 1980–1989, *J. Geophys. Res.*, *104*, 12,492–12,506, 1999.

St Cyr, O. C., et al., Properties of coronal mass ejections: SOHO LASCO observations from January 1996 to June 1998, *J. Geophys. Res.*, *105*, 18,169–18,185, 2000.

Tsurutani, B. T., and W. D. Gonzalez, The interplanetary causes of magnetic storms: A review, in *Magnetic Storms*, *Geophys. Monogr. Ser.*, vol. 98, edited by B. T. Tsurutani, W. D. Gonzalez, and Y. Kamide, p. 77, AGU, Washington, D. C., 1997.

Tsurutani, B. T., W. D. Gonzalez, F. Tang, S. I. Akasofu, and E. J. Smith, Origin of interplanetary southward magnetic fields responsible for major magnetic storms near solar maximum (1978–1979), *J. Geophys. Res.*, *93*, 8519–8531, 1988.

Tsurutani, B. T., W. D. Gonzalez, F. Tang, and Y. T. Lee, Great magnetic storms, *Geophys. Res. Lett.*, *19*, 73, 1992.

Wang, Y. M., S. Wang, and P. Z. Ye, Multiple magnetic clouds in interplanetary space, *Sol. Phys.*, *211*, 333–344, 2002a.

Wang, Y. M., P. Z. Ye, S. Wang, G. P. Zhou, and J. X. Wang, A statistical study on the geoeffectiveness of Earth-directed coronal mass ejections from March 1997 to December 2000, *J. Geophys. Res.*, *107*(A11), 1340, doi:10.1029/2002JA009244, 2002b.

Wang, Y. M., P. Z. Ye, S. Wang, and X. H. Xue, An interplanetary cause of large geomagnetic storms: Fast forward shock overtaking preceding magnetic cloud, *Geophys. Res. Lett.*, *30*(13), 1700, doi:10.1029/2002GL016861, 2003a.

Wang, Y. M., P. Z. Ye, and S. Wang, A probable interplanetary origin of great geomagnetic storm: Multiple magnetic clouds, *Chin. J. Geophys.*, in press, 2003b.

Webb, D. F., and R. A. Howard, The solar cycle variation of coronal mass ejections and the solar wind mass flux, *J. Geophys. Res.*, *99*, 4201–4220, 1994.

Webb, D. F., E. W. Cliver, N. U. Crooker, O. C. St. Cyr, and B. J. Thompson, Relationship of halo coronal mass ejections, magnetic clouds, and magnetic storms, *J. Geophys. Res.*, *105*, 7491, 2000.

Wolfson, R., and B. C. Low, Energy buildup in sheared force-free magnetic fields, *Astrophys. J.*, *391*, 353, 1992.

Zwickl, R. D., J. R. Asbridge, S. J. Bame, W. C. Feldman, J. T. Gosling and E. J. Smith, Plasma properties of driver gas following interplanetary shocks observed by ISEE-3, in *Solar Wind Five*, edited by M. Neugebauer, *NASA Conf. Publ. 2280*, 711, 1983.

S. Wang, Y. M. Wang, and P. Z. Ye, School of Earth and Space Sciences, University of Science and Technology of China, Jinzai Road 96, Hefei, Anhui 230026, China. (swan@ustc.edu.cn; wym@mail.ustc.edu.cn; pzye@ustc.edu.cn)